Radiation Pattern Verification of Active Antenna Systems Using Near-Field Measurements

Chang-Lun Liao

Abstract — Fifth-generation (5G) new radio and commercial networks are currently deployed by telecommunication service providers around the globe. A 5G active antenna system (AAS) consists of a passive antenna array, a transceiver front end, and a baseband unit—all integrated into a single module. As a consequence, the radio frequency ports of traditional base station antennas can be replaced with an Ethernet-based interface. New methods are needed to verify and optimize the antenna performance under these conditions. In this article, we propose an over-the-air (OTA) near-field method that makes it possible to measure and verify the radiation pattern of an AAS. A vector signal generator is used to provide a single-tone source at 3.5 GHz for a commercial passive base station antenna. To reconstruct both the near-field amplitude and the phase distribution of the near-field region of an antenna, we did the following. Two receiving paths to the vector network analyzer (with a reference antenna located at the back of the base station antenna) were combined with an existing probe antenna of the spherical near-field measurement system. This way, a far-field radiation pattern can be realized using near-field-to-far-field transformation methods. The radiation patterns, which are measured using the OTA mode near-field method, are consistent with conventional near-field methods for 5G sub-6 GHz radio units.

1. Introduction

Fifth-generation (5G) mobile networks have been deployed by telecommunications service providers worldwide since 2020. 5G new radio supports operation in two frequency ranges: the sub-6 GHz band and the millimeter-wave band. However, radio signals at millimeter-wave frequencies suffer from high path loss, which means that the cellular coverage distance is relatively short for a given signal-to-noise ratio (SNR). According to the standard formulation of the Friis equations, the received power is inversely proportional to the square of the distance between the transmitter and receiver. In addition, it is also dependent on the carrier frequency (which determines the wavelength of the signal) and the gains of the transmitting and receiving antennas [1]. This means that the millimeter-wave spectrum has a large continuous bandwidth available for high-speed data transmission but also has a severe propagation-loss problem. For this reason, antenna arrays are needed to concentrate the electromagnetic wave energy on the desired coverage area. This can be done more effectively by utilizing the directional characteristics of the radiation patterns of active antenna systems (AASs). A 5G AAS consists of a passive antenna array, a transceiver front end, and a baseband unit that are integrated into one module. This means that the traditional antenna radio frequency (RF) ports can be replaced with an Ethernet-based interface. Over-the-air (OTA) test methods have already become mandatory to determine and verify the radiation characteristics and transmission performance of AASs. Therefore, new measurement methods are urgently needed to measure and verify radiation patterns and system performance. There are three conventional OTA testing methods for evaluating 5G active AASs: direct far-field (DFF), compact antenna test range (CATR), and near-field range (NFR). These testing methods have been proposed and clearly defined for 5G RF conformance tests within the Third Generation Partnership Project [2−4]. The first method, DFF, is the most intuitive and straightforward OTA test system. The far-field distance criterion can be mathematically defined as $R > 2D^2/\lambda$, where D is the largest dimension of the antenna for the device under test (DUT) and λ is the wavelength.

Furthermore, the phase error should be less than $\pi/8$ radians (or 22.5° within the quiet zone range) to meet the minimum requirements for the far-field condition [5]. Because the wavelength of a millimeter-wave is very short, large antenna apertures are usually needed. This is problematic due to the more extensive test space needed to satisfy the far-field criteria. Hence, a larger anechoic chamber and more installed hardware will be needed in the future. Unfortunately, this test environment also increases the overall testing cost and path loss. Furthermore, the SNR deteriorates quickly, and the dynamic range is further reduced for such test systems. The second OTA method, CATR, is an indirect far-field range method. It can help meet the path loss criteria and enable economical deployment in indoor spaces. The CATR test system consists of a feed antenna and a parabolic reflector. The feed is located at the focal point of the reflector, where it generates a spherical wave front sent to the reflector, which produces a collimated beam (plane wave) in the direction of the DUT. This way, the far-field conditions within the quiet zone can be created [6, 7]. CATR is a standard solution for both signaling and nonsignaling test scenarios for the millimeter-wave band [8]. The third conventional OTA test method, NFR, involves measuring radiation patterns by sampling the amplitude and phase distributions in the antenna

Manuscript received 29 December 2022.

Chang-Lun Liao is with the Wireless Communications Laboratory, Chunghwa Telecom Laboratories, No. 99, Dianyan Road, Yangmei District, Taoyuan City, 326402, Taiwan; e-mail: clliao@cht.com.tw.

radiating near field (the Fresnel region). These are then converted into the far-field amplitude distribution via a mathematical near-field-to-far-field (NF-FF) transformation [9−13]. Depending on their scan geometry, the NFR method can be classified into planar, cylindrical, and spherical types matching the specific antenna configuration [14]. In addition, the NFR approach requires less space and therefore has the lowest path loss and largest dynamic range among all OTA test methods. In addition, it can use holographic back projection to help understand the amplitude and phase distribution of the electromagnetic fields in the near zone of aperture antennas, enabling both diagnosis and optimization [15]. This test method is suitable for antenna diagnostics in research-and-development testing and can accurately characterize the far-field radiation pattern. However, the method is also time consuming and more complicated for collecting near-field data and transforming near-field information into far-field radiation patterns. More specifically, when the near-field test requires many measurement points, it must enable a sampling interval of at least $\lambda/2$ for the band it operates in. The NF-FF transformation requires both amplitude and phase data. These are usually obtained by directly coupling the transmitted signal from vector network analyzer (VNA) RF internal sources when testing using traditional passive-mode antenna radiation pattern test methods. However, for 5G AAS performance measurements, no RF measurement port is available. A new mechanism is needed to enable phase recovery over the air and reconstruct the near-field data from noncoherent RF sources. Related phase recovery methods for near-field OTA measurement systems are reported in [16, 17]. The existing near-field OTA testing method is suitable primarily for RF transmission testing because the received radio signals are down-converted from their carrier frequencies. Consequently, the signals undergo digital signal processing, which makes it difficult to obtain precise RF data with this method. For NF-FF transformations, these measurements require a single-tone continuous-wave signal because a modulated signal introduces additional errors [18]. Here, we propose a VNA-based spherical near-field antenna measurement system for transmit-only AAS verifications. A comparison is made between the far-field pattern obtained using the OTA mode near-field and other conventional near-field methods.

2. Measurement System Setup and Testing

The wiring diagram of the OTA spherical near-field measurement setup is shown in Figure 1. The antenna under test (AUT) has no physical RF port; it was replaced with an Ethernet-based interface that enables beamforming operations and digital data links through common interfaces (e.g., the enhanced common public radio interface). Since the direct coupling of the RF signal as phase reference from the AAS transmission mode is not possible, a separate antenna is needed (reference antenna). This way, it is possible to perform phase recovery for the AUT over the air, together with the existing probe antenna using spherical near-field measurement systems. Then the near-field amplitude and phase of the fields in the near-field region of the antenna can be reconstructed. First, we utilized a 20 dB directional coupler as a conduction mode to ensure the stability of the near-field data capture before starting the OTA mode near-field scan. The test range utilizes a theta-over-phi step motor positioning system. The probe antenna is mounted at the end of a fiberglass swing arm that can change the theta axis from 0° to 165°. It includes a support post for the AUT mount and motion about the phi axis from −180° to 180° during spherical scanning. In addition, the AAS must be able to transmit a single-tone continuous-wave signal. Then the reference and probe antenna for this test architecture can serve as reference and test paths, respectively. Both are connected via an RF cable to the input port 2 of the vector network analyzer. Consequently, an NF-FF transformation can be performed using two receiving paths for the radiation pattern measurement. The standard NF-FF transformation technique, based on spherical wave expansion, is applicable to both conventional and OTA mode near-field measurements. More specifically, the difference between them lies mainly in the phase reference mechanism used during the measurement process. However, the general steps involved in the NF-FF transformation process are the same for both cases. These steps include measuring the near-field data, processing and calibrating the data, transforming the near-field data to the far field, and reconstructing the far-field radiation pattern [19].

Figure 2 shows the proposed near-field setup for the beamforming pattern measurement. The distance between the AUT and probe antenna is about 120 cm, and the scan range is constant. The reference antenna consists of cross-dipole structures with two RF ports. One of the RF ports in the reference antenna that matches the polarization of the AUT is selected, while the other port is terminated with a 50 ohm load. The reference antenna is placed adjacent to the back of the AUT (within about 10 cm), and the position is fixed in the same coordinate frame for AUT placement. Hence, there is no relative motion between the AUT and the reference antenna. A simple block diagram indicates that the receiving part has digitized intermediate-frequency ratios between the test and the reference channel. The vector network analyzer combines all components into a single unit. Note that a vector network analyzer is often used for antenna radiation pattern measurement setups for passive antennas. The vector network analyzer generates the source signal for conventional near-field measurements and serves as a receiver that determines both magnitude and phase data against its reference signal [20].

Figure 3 shows conventional and proposed OTA near-field measurement systems. The conventional system typically uses a VNA with an internal signal source.

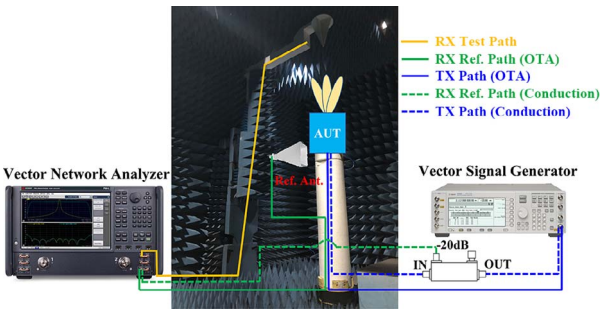

Figure 1. Wiring diagram of the OTA spherical near-field measurement system.

The VNA sweeps a frequency range and measures the complex reflection coefficient or S-parameters of the AUT at each measurement point. In contrast, the OTA mode near-field measurement system uses an external noncoherent source, such as a signal generator, to provide a known incident field on the AUT. The main advantage of using an OTA near-field measurement system is that it allows for testing of the device in a more realistic environment (electromagnetic fields come from an external noncoherent source).

A commercial passive base station antenna (model S4-90M-R1-V2, an eight-port planar array antenna system with a frequency range of 3300 MHz to 3800 MHz, made by CommScope, Inc. [21]) was built to measure the radiation pattern performance using the OTA spherical near-field method. To determine the beamforming characteristics, the commercial base station antenna had four columns arranged in a linear array that can provide 8T8R beamforming functions. This is usually combined with a baseband weighting configuration and an adaptive algorithm from the radio access network equipment to send a narrow beam toward the user equipment. This further improves the signal-to-interference-and-noise ratio within areas with cellular coverage. In addition, the baseband can use different RF channel weightings, including the amplitude and phase of the signals, for each RF port. This way, it becomes possible to generate specific patterns and directions for the service beam, which enables the

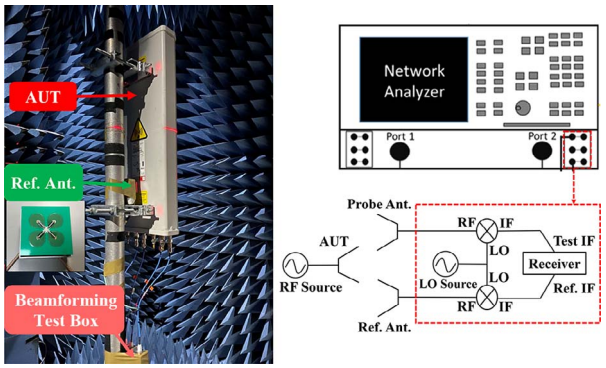

Figure 2. Setup of the proposed near-field OTA method for beamforming pattern measurements.

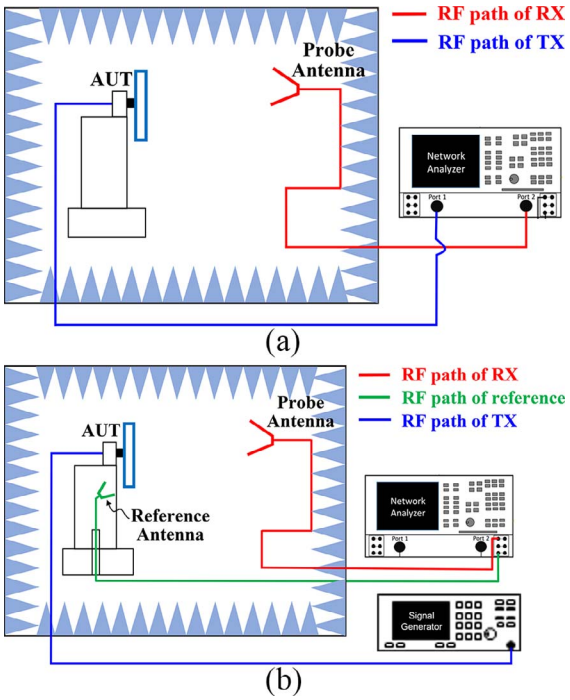

Figure 3. Schematic of a near-field measurement system for (a) conventional and (b) proposed OTA modes.

determination of the 5G coverage area between the base transceiver station and the user equipment terminal. Two different beamforming test boxes were used: one uses a service beam (30°), while the other uses a soft split beam (24°). Both are from CommScope, Inc., and are equipped with a base station antenna. This was done to obtain the beamforming statuses for the near-field tests. The AUT construction is shown in Figure 4. Each beamforming test box consists of a one-to-four power divider with an RF jumper cable. Both produce the amplitude and phase distributions of the RF signals, synthesizing specific beamforming patterns. Four RF input ports of the beamforming test box are connected with the base station antenna ports of the same polarization interface. This is done such that all are connected to $+45°$ polarization ports, while the remaining four $-45°$ polarization ports are terminated with a 50 ohm load and vice versa. Finally, the output port of the beamforming test box is directly connected to the vector signal generator through an RF cable.

3. Results

The beamforming pattern measurements of the base station antenna are analyzed using the two beamforming test boxes. In order to enable a comparison with the OTA near-field method, the conventional near-field method was also used to determine the radiation patterns. For these two near-field measurements, the radiation patterns in two principal planes (using the service beam 30° and soft split beam 24° beamforming test boxes) are, respectively, shown in

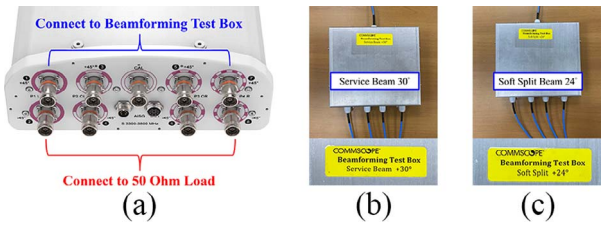

Figure 4. Beamforming pattern test verification for two different beamforming statuses. (a) Port configuration of a commercial passive base-station antenna, (b) service beam 30°, and (c) soft split beam 24°.

Figure 5 and Figure 6. The blue dashed line in both plots shows the OTA mode near-field method results, while the red line represents the conventional near-field methods. Clearly, the radiation patterns for co-polarization and cross-polarization on H-cut and V-cut planes at 3.5 GHz are consistent for both test methods. To obtain accurate results using both methods, it was important to control the testing environment carefully. This involved ensuring that the reference channel was stable, enabling excellent phase recovery in OTA mode, and the SNR was sufficient throughout the testing system. We also minimized external interference and ensured that the radiation patterns of the AUT were reflected accurately.

4. Conclusions

We investigated a novel OTA near-field method to measure single-tone transmit-only AAS radiation patterns. Using a vector signal generator, a commercial passive base station antenna was fed with signals from two different beamforming test boxes. This was done to model and measure the AAS for single-tone source

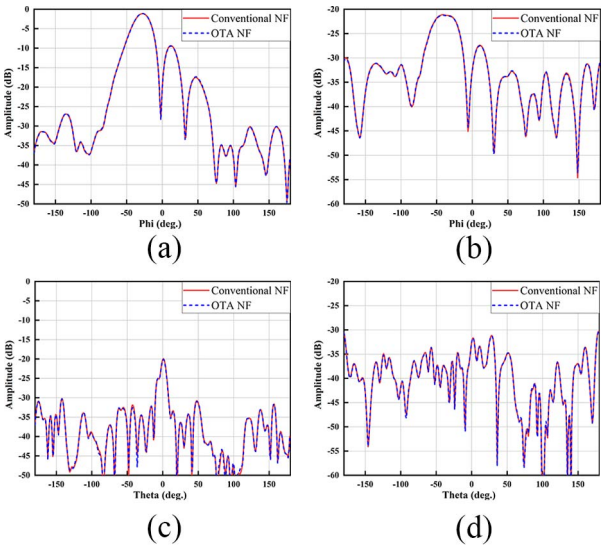

Figure 5. Comparison of the radiation patterns using the service beam 30° beamforming test box for the (a) co-polarization of the H-cut plane, (b) cross-polarization of the H-cut plane, (c) co-polarization of the V-cut plane, and (d) cross-polarization of the V-cut plane for both the OTA near-field and the conventional near-field methods.

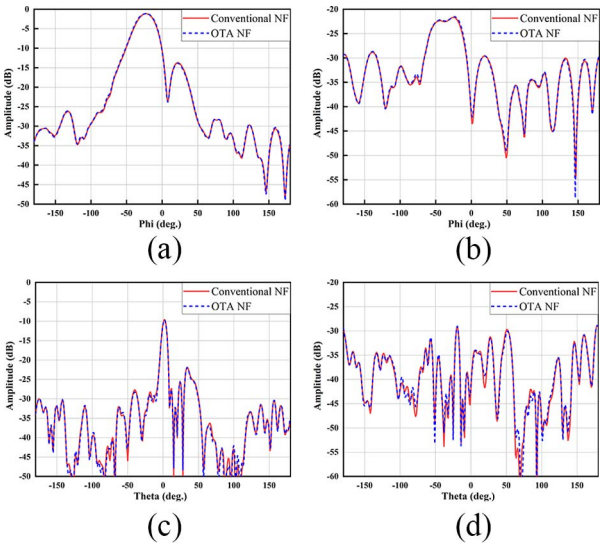

Figure 6. Comparison of the radiation patterns using the soft split beam 24° beamforming test box for the (a) co-polarization of the H-cut plane, (b) cross-polarization of the H-cut plane, (c) co-polarization of the V-cut plane, and (d) cross-polarization of the V-cut plane for both the OTA near-field and the conventional near-field methods.

transmission. The obtained radiation patterns with the new OTA near-field method were consistent with the conventional near-field test results for 5G sub-6 GHz radio units.

5. Acknowledgments

The author would like to thank CommScope, Inc., for providing the commercial base station antenna and the beamforming test boxes to conduct the near-field measurements. Special thanks to the National Taiwan University of Science and Technology and WaveFidelity Inc. for their valuable technical support that helped build the OTA near-field system.

6. References

1. D. C. Hogg, “Fun With the Friis Free-Space Transmission Formula,” *IEEE Antennas and Propagation Magazine*, **35**, 4, August 1993, pp. 33-35, doi: 10.1002/dac.1348.
2. ETSI, “Universal Mobile Telecommunications System (UMTS); LTE; 5G; Radio Frequency (RF) Conformance Testing Background for Radiated Base Station (BS) Requirements (3GPP, TR 37.941 v16.3.0 Release 16.3.0),” https://www.etsi.org/deliver/etsi_tr/137900_137999/137941/16.03.00_60/tr_137941v160300p.pdf, 2021.
3. I. R. R. Barani, L. A. Bronckers, and A. C. F. Reniers, “Integrated-Antenna Over-the-Air Testing for Millimeter-Wave Applications: An Overview of Systems and Uncertainty [Measurements Corner],” *IEEE Antennas and Propagation Magazine*, **64**, 5, October 2022, pp. 97-110, doi: 10.1109/MAP.2022.3195469.
4. H. Kong, Z. Wen, Y. Jing, and M. Yau, “Midfield Over-the-Air Test: A New OTA RF Performance Test Method for 5G Massive MIMO Devices,” *IEEE Transactions on Microwave Theory and Techniques*, **67**, 7, July 2019, pp. 2873-2883, doi: 10.1109/TMTT.2019.2912369.

5. B. Derat, G. F. Hamberger, and F. Michaelsen, "On the Minimum Range Length for Performing Accurate Direct Far-Field Over-the-Air Measurements," 2019 Antenna Measurement Techniques Association Symposium (AMTA), San Diego, CA, USA, October 06-11, 2019, doi: 10.23919/AMTAP.2019.8906460.
6. L. M. Tancioni, A. Jernberg, P. Noren, A. Giacomini, A. Scannavini, et al., "Over-the-Air Testing of Active Antenna System Base Stations in Compact Antenna Test Range," 2019 13th European Conference on Antennas and Propagation (EuCAP), Krakow, Poland, 31 March - 05 April, 2019.
7. H. Gao, F. Zhang, G. F. Pedersen, and W. Fan, "A Fast Multibeam Measurement Method for Millimeter-Wave Phased Arrays," *IEEE Antennas and Wireless Propagation Letters*, **21**, 7, July 2022, pp. 1502-1506, doi: 10.1109/LAWP.2022.3174246.
8. C. Rowell, B. Derat, and A. C. García, "Multiple CATR Reflector System for Multiple Angles of Arrival Measurements of 5G Millimeter Wave Devices," *IEEE Access*, **8**, November 2020, pp. 211324-211334, doi: 10.1109/ACCESS.2020.3038597.
9. P. Shen, Y. Qi, W. Yu, J. L. Drewniak, M. Yu, et al., "An RTS-Based Near-Field MIMO Measurement Solution—A Step Toward 5G," *IEEE Transactions on Microwave Theory and Techniques*, **67**, 7, July 2019, pp. 2884-2893, doi: 10.1109/TMTT.2019.2901687.
10. F. R. Varela, B. G. Iragüen, and M. S. Castañer, "Fast Spherical Near-Field to Far-Field Transformation for Offset-Mounted Antenna Measurements," *IEEE Antennas and Wireless Propagation Letters*, **19**, 12, December 2020, pp. 2255-2259, doi: 10.1109/LAWP.2020.3029605.
11. F. D'Agostino, F. Ferrara, C. Gennarelli, R. Guerriero, M. Migliozzi, et al., "A Useful Sampling Representation for Mapping the Antenna Near-Field," *IEEE Open Journal of Antennas and Propagation*, **2**, June 2021, pp. 709-717, doi: 10.1109/OJAP.2021.3085508.
12. A. G. Toshev, "Application of Fourier Integrals for Determination of Antenna Far-Field Patterns From Measurements at Fresnel Distances," *IEEE Transactions on Antennas and Propagation*, **65**, 4, April 2017, pp. 1700-1705, doi: 10.1109/TAP.2017.2671034.
13. Y. Qi, G. Yang, L. Liu, J. Fan, A. Orlandi, et al., "5G Over-the-Air Measurement Challenges: Overview," *IEEE Transactions on Electromagnetic Compatibility*, **59**, 6, December 2017, pp. 1661-1670, doi: 10.1109/TEMC.2017.2707471.
14. L. J. Foged, M. H. Francis, and V. Rodriguez, "Update of IEEE Std 1720-2012 Recommended Practice for Near-Field Antenna Measurements," 2019 Antenna Measurement Techniques Association Symposium (AMTA), San Diego, CA, USA, October 06-11, 2019, doi: 10.23919/AMTAP.2019.8906313.
15. L. J. Foged, F. Mioc, A. Rosa, "Applicability Investigation of Holographic Back-Projection of Spherical Near Field Measured Data," 2006 First European Conference on Antennas and Propagation, Nice, France, November 06-10, 2006, doi: 10.1109/EUCAP.2006.4584680.
16. B. Fourestie, J. C. Bolomey, T. Sarrebourse, Z. Altman, J. Wiart, "Spherical Near Field Facility for Characterizing Random Emissions," *IEEE Transactions on Antennas and Propagation*, **53**, 8, August 2005, pp. 2582-2589, doi: 10.1109/TAP.2005.851847.
17. T. Kawamura and A. Yamamoto, "Near-Field Measurement System for 5G Massive MIMO Base Stations," *Anritsu Technical Review*, **25**, September 2017.
18. B. T. Walkenhorst, "Test Environments for 5G Millimeter-Wave Devices," 2019 13th European Conference on Antennas and Propagation (EuCAP), Krakow, Poland, 31 March - 05 April, 2019.
19. IEEE, "IEEE Recommended Practice for Near-Field Antenna Measurements," https://ieeexplore.ieee.org/document/6375745, December 5, 2012.
20. IEEE, "1720-2012—IEEE Recommended Practice for Near-Field Antenna Measurements," December 2012, doi: 10.1109/IEEESTD.2012.6375745.
21. CommScope, Inc, "S4-90M-R1-V2: 8-Port Planar Array Antenna, 3300−3800 MHz, 90° HPBW, 1× RET," https://www.commscope.com/globalassets/digizuite/263529-p360-s4-90m-r1-v2-external.pdf.